ISSN-1996-918X

Pak. J. Anal. Environ. Chem. Vol. 14, No. 1 (2013) 54 – 60

Reduction of Hexavalent Chromium Using L-Cysteine Capped Nickel Nanocatalysts

Nazar Hussain Kalwar[1], Sirajuddin[1*], Syed Tufail Hussain Sherazi[1], Abdul Rauf Khaskheli[2], Razium Ali Soomro[1] and Afzal Shah[3]

[1]*National Centre of Excellence in Analytical Chemistry, University of Sindh, Jamshoro-76080, Pakistan*
[2]*Department of Pharmacy, Shaheed Mohtarma Benazir Bhutto Medical University, Larkana- 77150, Pakistan*
[3]*Department of Chemistry, University of Science & Technology, Bannu, 28100, (KPK), Pakistan*

Received 05 July 2012, Revised 03 March 2013, Accepted 06 June 2013

Abstract

The aim of this study was to reduce the highly toxic hexavalent chromium Cr(VI) into less toxic chromium Cr(III) species by using nickel nanoparticles (Ni NPs) as catalysts in order to provide safety to the aqueous environment. In the first phase Ni NPs were synthesized in ethylene glycol and capped with l-cysteine by a modified microwave irradiation method using NaOH as the accelerator. The formed Ni NPs were characterized by various techniques such as UV-Visible spectroscopy, Fourier Transform Infra-red (FTIR) spectroscopy and Scanning Electron Microscopy (SEM). In the second phase the formed Ni NPs were immobilized on glass surfaces and employed as catalyst for the reduction of Cr(VI) ions. According to observations, 99% reduction of Cr(VI) ions was achieved in the presence of 0.5 mg of Ni NPs catalyst in just five minutes as compared to nickel powder that showed only 16% reduction in 15 minutes. The study has a great impact on the aqueous pollution control of Cr(VI) especially caused by the discharge of waste water from several industries utilizing Cr(VI) containing salt as one of the essential gradients.

***Keywords*:** Nickel Nanocatalyst; L-Cysteine; Hexavalent Chromium; Reduction.

Introduction

The release of heavy metals into aquatic environment has continuously been increasing by disposal of industrial sludge/effluents. This practice donates major hazards to the environment and ultimately endangers human health due to their accumulation in food chain, water channels and persistence in nature [1]. Among several heavy metals chromium is known as one of the very toxic constituents of the water systems. This enters into water bodies via several industries like textile, leather tanning, steel production, electroplating, anodizing of aluminum, water cooling, wood preservation and chromate preparation [2]. The chromium is mainly found in two typical oxidative states, hexavalent Cr(VI) and trivalent Cr(III). These oxidation states have tremendous contrast in their transport characteristics and toxicity properties. Hexvalent chromium is extremely toxic with more water solubility and improved mobility, while trivalent chromium is less toxic due its lesser solubility and poor mobility in water systems [3-4]. Concerning the solution pH values, Cr(VI) may exist in many forms like chromate (CrO_4^{2-}), dichromate ($Cr_2O_7^{2-}$) and hydrochromate ($HCrO_4^-$), while Cr(III) contains hydrated trivalent forms like $Cr(H_2O)_6^{3+}$ and chromium hydroxide complexes, $Cr(OH)_2(H_2O)_4^+$ or $Cr(OH)(H_2O)_5^{2+}$. Several reports suggest the lesser adsorption efficiency of Cr(VI) onto the negatively charged soil particles is due to its strong electro active

*Corresponding Author Email: drsiraj03@yahoomail.com

repulsive force. Therefore, it can freely enter and move in water systems [4-5]. Conversely Cr(III) species hold positive electric charges and thus can easily be deposited on negatively charged soil particles [5-6].

A number of decontamination methods for remediation of heavy metal ions and other toxic substances from industrial effluents have been proposed such as electro-coagulation, electro-wining, electro-dialysis, ion exchange, precipitation and reverse osmosis [6]. However, these remediation approaches have potential disadvantages namely high energy or reagent requirements, incomplete removal of pollutants and generation of other waste products and toxic sludge. Together with these removal methodologies are usually too expensive if contaminants are in a very low concentration range 10-100 mg/L. On the other hand, inexpensive, rapid and simple treatment procedures are required and preferred for removal or remediation of contaminated waters [7]. Many workers have explained the toxicity of Cr(VI) to be mainly due to formation of transitional Cr oxidation states like Cr(V), Cr(IV) and finally Cr(III) [7-8]. Although no toxic effects have been reported for in vivo studies of Cr(III), it can react with DNA and protein molecules on entering into the cell and make stable bonds because of its brutal reactivity with oxygen, nitrogen and sulfur on a few binding sites [8]. Additionally Cr(III) is very inactive and therefore it is taken as a dietary supplement in the form of Cr picolinate that has been observed to possess no adverse effects at the suggested intake level. However, reports also show that higher intakes of Cr(III) than the recommended levels lead to adverse effects, though Cr(III) alone cannot be solely blamed for reported toxicities, because many other moieties could add undesirable effects. Numerous works have been published that demonstrate beneficial consequences of Cr(III) species during supplementation in individuals by means of impaired glucose tolerance [8]. Henceforth, major scientific consensus is that Cr(VI) is considerably more toxic than Cr(III). It is also argued that if all ingested Cr(VI) could convert to Cr(III) inside the stomach, then it should be concluded that humans may tolerate intensive levels of Cr(VI) exposure. Moreover, standards for drinking water concentration of Cr(VI) are set as 50-100 µg/L by the World Health Organization and almost every other state agency like, the US Environmental Protection Agency [9]. Studies show that 50-100 µg/L Cr(VI) is not a small concentration and equates to nearly 1-2 µM of Cr(VI) availability into water systems [8].

The photo-catalytic reduction of pollutants mainly occurs due to the excitation of valence band electrons to the conduction band that is initiated through light absorption. In result, region of excited electrons and holes are generated which are responsible for oxidation and reduction process. [10-12]. Many studies have been devoted to explain the use of excited holes to oxidize pollutants in the presence of SO_4^{2-}/TiO_2 catalysts, where excited electrons have been utilized in photo-reduction reactions [13]. In addition, it is still unclear whether the efficiency of photo-catalysis is influenced by structural properties of the catalysts [14]. Nanocomposite materials have been given tremendous scientific importance because they hold high potential for catalytic applications. A large volume of nanoscale composite is formed of small grain sizes. Therefore a significant fraction of nanocomposite material contains interface/grain boundaries at the atomic level [15]. Nanoscale nickel particles have found applications in many fields like mechanics, electronics, sensors and catalysis. Similarly, it has also been observed that exposed surface area contributes a key role in catalysis and therefore nanosized materials are used for this purpose. Here we address the use of Ni NPs formed by an improved microwave assisted digestion method using l-cysteine as a capping material and their use as highly efficient catalyst for reduction of Cr(VI) in aqueous medium.

Materials and Methods

Chemicals and reagents

L-cysteine ($C_3H_7NO_2S$), nickel chloride ($NiCl_2.6H_2O$), sodium carbonate (Na_2CO_3), sodium hydroxide (NaOH), ethanol (C_2H_5OH), ethyleneglycol (CH_2OHCH_2OH) were all obtained from Fluka Chemicals. All the chemicals were analytical grade and used as received.

Washing of glassware and preparation of stock solutions

All glassware was cleaned with detergent containing water followed by washing several times with tap water and finally rinsed with deionized water. All the glassware was then dried in an oven at 100 °C and used for solution preparation. Stock solutions of cysteine (0.01 M) and $NiCl_2.6H_2O$ (0.01 M) were prepared in ethylene glycol while the sodium carbonate (0.1 M), sodium hydroxide (0.1 M) and HCl (0.1 M) were prepared in deionized water by using their desired quantities in different volumes.

Synthesis of cysteine-capped Ni NPs

In a typical experiment, synthesis of nickel nanoparticles was carried out by mixing 1 ml nickel chloride with 0.6 ml l-cysteine followed by adding 0.3 ml sodium carbonate and 0.1 ml sodium hydroxide. The mixture was diluted with ethylene glycol to make a total volume of 6.0 ml. It was then poured into a conical flask of 25 ml capacity and exposed to microwave irradiation (Glanz, 900W) for 60 s (six periods of 10 s each); during this time the light green solution turned to black. The as obtained black colloidal dispersion of microwave irradiated Ni NPs sample was put into an ice water bath to promptly cool down the products to room temperature in order to avoid the aggregation of NPs and UV-Visible spectra were recorded. A similar procedure was followed for sample preparation throughout the optimization and application studies. Further, the characterization studies were carried out using various techniques as discussed in the results and discussion section.

Procedure for catalytic test

In a typical experiment, 0.4 ml of 100 µg/ml Cr(VI) solution was put into a quartz cell and diluted to 4.0 ml by adding 3.6 ml of deionized water for recording the UV-Visible spectra. This solution was prepared to check the absorption profile of Cr(VI) species in the aqueous medium which showed a prominent absorption peak at 352 nm for Cr(VI) ions. Simillarly, a 4.0 ml solution was prepared by taking 10 µg/ml Cr(VI) ions and 0.1 M $NaBH_4$. Another experiment was carried out using similar concentrations of the reactants in the presence of 0.5 mg of bulk nickel powder (raney nickel) as catalyst. Finally, we carried out the experiment for catalytic reduction of Cr(VI) by adding 0.5 mg of nanosized nickel particles (as catalysts deposited on pieces of glass cover slip) that resulted in 99% reduction in a very short time (5 minutes). The glass cover slips were weighed before and after loading the catalysts already prepared in colloidal dispersions to find out the amount of catalyst deposited on pieces of cover slips.

Results and Discussion

UV-Visible spectroscopy

The study for surface plasmon resonance of l-cysteine capped Ni NPs synthesized by the microwave assisted method was performed using a UV-Visible spectrophotometer model Lambda 2 of Perkin-Elmer, Germany. Several experiments were performed to optimize different parameters for better and reproducible synthesis of Ni NPs in ethylene glycol. A representative UV-Visible spectrum for the prepared l-cysteine capped Ni NPs is shown in (Fig. 1a). This was obtained from a sample prepared after all the optimized parameters were optimized in the procedure for synthesis of Ni NPs.

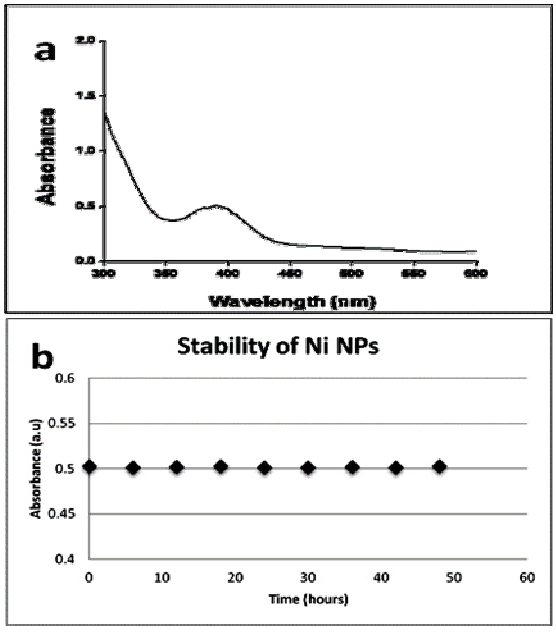

Figure 1. **UV-Visible spectrum recorded for (a) l-cysteine capped Ni NPs obtained at pH 7.4 with 1:6 molar ratio of Ni to l-cysteine and (b) plot of absorbance v/s time for stability of Ni NPs at λmax of 386 nm.**

The UV-Visible spectrum recorded for a typical sample show an absorbance maximum at 386 nm wavelength which corresponds to the formation of Ni NPs. Optimization studies of many parameters such as reducing and capping agent concentration, quantity of precursor, sodium carbonate, sodium hydroxide and hydrochloric acid were performed and additional experiments carried out to check the effect of time and pH after optimization studies also demonstrated the stability of nanosized metal products as shown in (Fig. 1b). The nickel ions must have been reduced by hydrazine hydrate because it is a strong reducing agent and reaction would have followed the similar reduction path as mentioned elsewhere [16]. We believe that encapsulation of the freshly prepared l-cysteine derived Ni NPs must also followed the similar patterns to those discussed by other workers [17].

FTIR Spectroscopy

The FTIR spectra of standard l-cysteine amino acid and S-linked l-cysteine capped Ni NPs have been presented in (Fig. 2). These FTIR spectra were recorded to verify the binding interaction of l-cysteine molecules with nanoparticle surfaces.

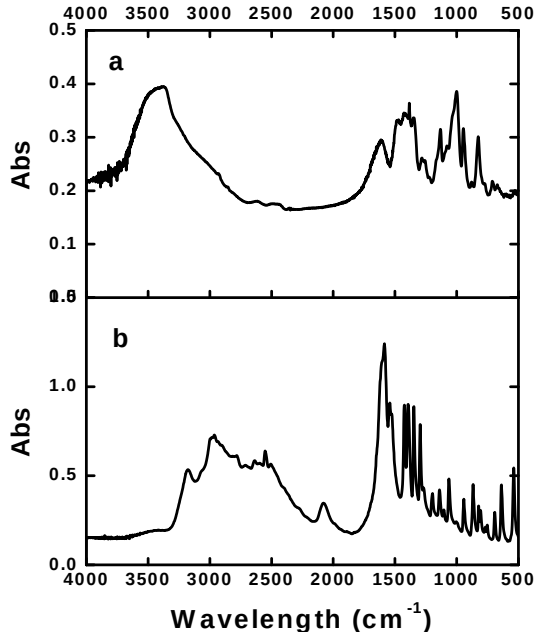

Figure 2. **FTIR spectra of (a) newly synthesized Ni NPs and (b) pure l-cysteine.**

(Fig. 2b) shows a characteristic absorption band at 2551 cm^{-1} (i.e. in the range 2600-2550 cm^{-1}) which is assigned to an S-H stretching vibration of standard l-cysteine [17]. This band disappears on encapsulation of Ni NPs with l-cysteine molecules as depicted in (Fig. 2(a)), reporting the strong surface binding interactions of amino acid molecules via thio linkage to the particle surfaces. This is also in good agreement with work already reported [17, 18].

Further, it is observed from FTIR spectral study that bands at 1585 cm^{-1} and 1544 cm^{-1} were appeared in free l-cysteine molecules; these are attributed to formation of $–CO-NH_2$ linkages between amino acid molecules (on the surface of different nanoparticles), and shifted to 1608 cm^{-1} and 1578 cm^{-1} respectively (in this case). Therefore, we argue that l-cysteine molecules do not interact via the carboxylate group whereas the shifts in signals provide a hint to the surface interactions due to the -S group via thiolate linkage [19]. Further confirmation of the argument is evidenced by the disappearance of diagnostic peak for $–NH_3^+$ in a newly synthesized Ni NPs sample that appeared prominently at 2080 cm^{-1} in FTIR spectra of standard l-cysteine which is assigned to formation of acylamino groups due to zwiterionic moieties [17].

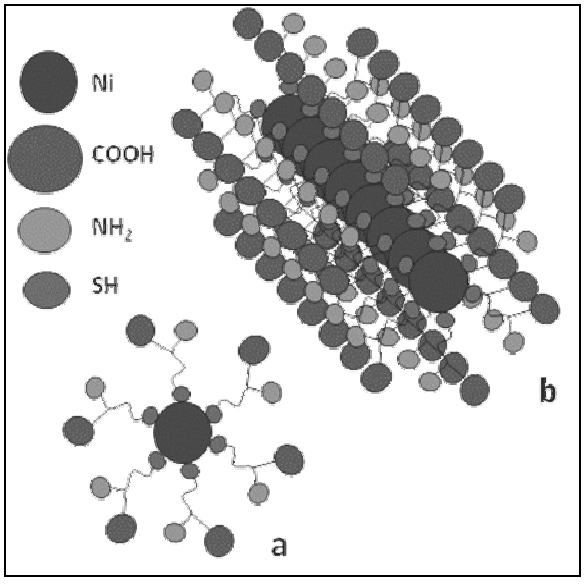

Figure 3. **Schematic formations of (a) spherical Ni nanoparticles and (b) Ni nanorod via different linkages.**

In addition the strong and broad signal in the spectral range 2300-3400 cm^{-1} appears due to the collective effect of intermolecular H-bonding between –OH and $–NH_2$ groups of the l-cysteine molecules. The shift of these signals to higher frequencies is simply because of newer binding interactions between nanoparticle surfaces and amino acid molecules as shown in (Fig. 3).

Illustrations discussed so far strengthen the proposed structures of spherical and longitudinal shapes of l-cysteine capped Ni NPs which can be presented by the schematic diagram shown in (Fig. 3).

Scanning electron microscopy (SEM)

An SEM study was carried out to investigate surface characteristics such as morphology and size of the synthesized l-cysteine capped Ni NPs in ethylene glycol and typical SEM image is shown in (Fig. 4).

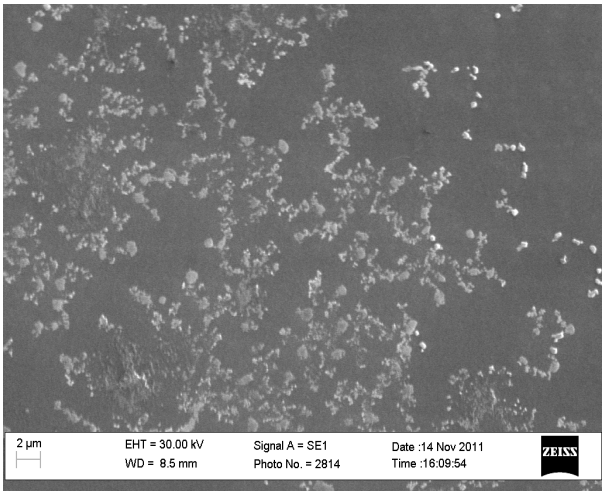

Figure 4. **SEM image of newly synthesized cyst-Ni NPs by microwave irradiation in ethylene glycol.**

The image shown in (Fig. 4) was recorded for optimized samples of Ni NPs with 1:6 molar ratio of Ni to cysteine. It is clearly shown that most of the particles are smaller in size but with the exception of a very small contribution from aggregated Ni NPs. The small degree of aggregation is perhaps due to possible intra molecular interactions and peptide bond formation between l-cysteine molecules bound with surface of Ni NPs. Close examination of these images reveals that most of the smaller particles are rod/chain shaped with a few spherical particles. The small sized nanoparticles can be separated from aggregated ones by passing the sample solution through a nanofiltration membrane with a mesh size of 50-200 nm. This serves as the template to form l-cysteine capped Ni NPs with different morphologies. The average size of spherical nanoparticles was 14 nm in the range of 5–35 nm while that of the nanorods/chains was 20 nm x 60 nm with a range of 5 nm x 10 nm–50 nm x 120 nm. These smaller nanospheres and nanorods/chains promise good catalytic activity for some specific applications. A number of methods have been reported for synthesis of Ni NPs, though few synthesized Ni NPs and characterized by SEM [16, 20].

Catalytic activity of Ni NPs for reduction of Cr (VI) ions

The investigation for catalytic behavior of l-cysteine derived Ni NPs was monitored by UV-Visible spectroscopy. Experiments were carried out to check the efficiency of nanocatalysts using potassium dichromate ($K_2Cr_2O_7$) as a model compound and sodium borohydride as the reducing agent while the newly synthesized Ni NPs were employed as catalysts during the method. We checked different parameters which influence the reduction of Cr(VI) species such as concentration of potassium dichromate, sodium borohydride, quantity of Ni NPs and reaction time. In a typical experiment 10 µg/ml Cr(VI) solution was treated with 0.1 M $NaBH_4$ in the presence and absence of Ni powder and Ni NPs in a quartz cell and spectra recorded in the range of 300-500 nm. The results are presented in (Fig. 5). This shows a broad and clear absorption peak for Cr(VI) ions in aqueous medium with a characteristic λ_{max} of 352 nm, which on addition of $NaBH_4$ shifts to longer wavelength with an enhanced absorption peak at λ_{max} of 372 nm. This change in absorption profile can be attributed to a change in pH of the solution after addition of $NaBH_4$. We observed that the pH of the solution was 6.9 before and 9.7 after addition of $NaBH_4$. This pH change caused change in the absorption maximum for the Cr(VI) moieties as shown in (Fig. 5a). Further we observed a very small decrease in the absorbance at 372 nm which is due to the reduction of Cr(VI) ions produced by

$NaBH_4$ alone in aqueous medium without the addition of any catalyst. Catalytic reduction of Cr(VI) to Cr(III) is carried out through excited electrons initiated by hydride ions in presence of UV-Visible irradiation such that over all catalytic reduction of Cr(VI) is illustrated by the equations below. Further we studied experimental findings for nanoparticle catalyzed reduction of Cr(VI) with strong reducing agent (i.e. $NaBH_4$) under UV-Vis irradiation as shown in (Fig. 5) that may also follow same pathway during the course of reaction.

Scheme 1

$$Cr_2O_7^{2-} + 14H^+ + 6e^- \xrightarrow{\text{nanoparticles}} 2Cr^{3+} + 7H_2O \quad (4)$$

$$2H_2O + 4h^+ \rightarrow O_2 + 4H^+ \quad (5)$$

The time profiles demonstrated in figure 5, for remediation of Cr(VI) ions from an aqueous solution catalyzed by l-cysteine derived Ni NPs, presents a clear picture of high catalytic activity of the nanosized nickel catalysts as compared to that of reduction performed without catalyst and in the presence of metallic nickel powder. The UV-Visible spectra show marked differences in catalytic efficiencies produced by the metallic nickel powder and nanocatalyst during the course of reduction. Specific surface area, crystalline nature and crystalline phases have generally been believed to be the important factors for controlling activity of catalysts [21]. However the nanocatalysts possess large specific surface areas which imply high adsorption capacities for the analytes. These large surface areas, in principle are responsible for the rapid and efficient catalytic reduction of Cr(VI) in the present study [14].

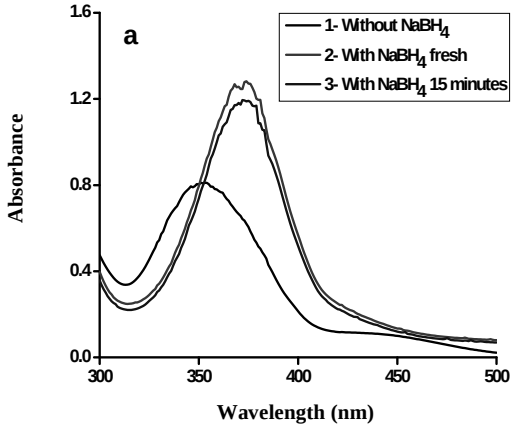

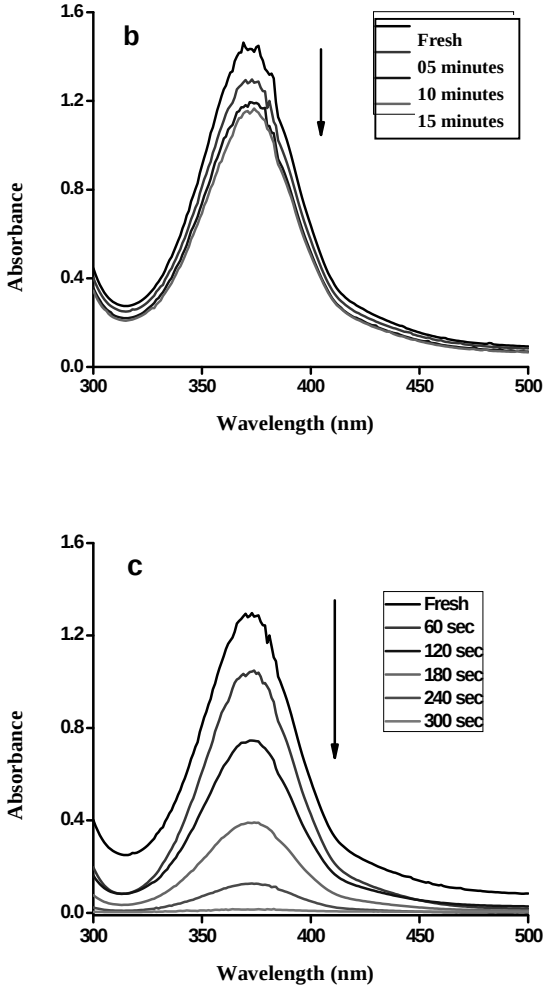

Figure 5. **UV-Visible spectra of Cr(VI) a) 10 µg/ml Cr(VI) ions in water, 1, without addition of $NaBH_4$ a peak at 352 nm, 2, after addition of 0.1 M $NaBH_4$ (fresh solution) and 3, same as 2 but after 15 min; b) reduction of Cr (VI) with 0.1 M $NaBH_4$ in the presence of 0.5 mg Ni powder, where UV-Vis spectra were recorded after 5 min up to a time of 15 min and c) same as b) but using Ni NPs instead of Ni powder and spectra recorded after 60 sec each which showed nearly complete reduction of Cr(VI) ions in a very short time.**

In particular, there was only 6% reduction of Cr(VI) ions (in absence of any catalyst) after 15 minutes times, as calculated from absorption results from the UV-Visible spectra after addition of $NaBH_4$ alone. We also performed experiments to reduce Cr(VI) ions with $NaBH_4$ in the presence of Ni powder as catalyst, which resulted in 23% reduction in 15 minutes as shown in figure 5(b). Similar experiments were also carried out to check the catalytic activity of newly synthesized l-cysteine capped Ni NPs. For this we used the same concentrations of the model reagent and reducing

agent, and observed 99% reduction of Cr(VI) ions in a very short time as illustrated in Figure 5(c). The reduction of Cr(VI) can be described as:

Scheme 2

$$2K_2Cr_2O_7 + 2NaBH_4 \longrightarrow 2Cr_2O_3 + 4KOH + 2NaOH + 2B(OH)_3$$

In this case a maximum reduction of 99% was recorded for Cr(VI) ions. These results prove a clear picture of the difference in size between Ni powder and Ni NPs and their use as reduction catalysts. The reduction of Cr(VI) has not been previously studied by using Ni NPs but Pd NPs [22] and Fe_2O_3 stabilized Fe^0 NPs [23] have been used as efficient catalysts for this purpose.

Conclusion

The current study has shown that l-cysteine capped Ni NPs are excellent catalysts for almost complete remediation of hexavalent chromium ions from aqueous environments. We observed 99% reduction of Cr(VI) ions with Ni NPs in a very short time (greater than four times increase in reduction was achieved in three fold lesser time) compared to using conventional nickel powder as catalyst. These nanosized catalysts were prepared in ethylene glycol by microwave assisted reduction of nickel chloride with hydrazine hydrate and used as heterogeneous catalysts for reduction of Cr(VI) ions by depositing on glass cover slips. We observed that l-cysteine capped Ni NPs have not been used for similar reduction/ remediation studies of hexavalent chromium species and also predict that the current study is expected to open new doors for their further application in other experiments of environmental importance.

References

1. M. Gavrilescu. *Engineering Life Science,* 4 (2004) 219.
2. U. K. Garg, M. P. Kaur, V. K. Garg and D. Sud. *J. Hazard. Mater.,* 140 (2007) 60.
3. Sirajuddin, L. Kakakhel, G. Lutfullah, M. I. Bhanger, A. Shah and A. Niaz, *J. Hazard. Mater.,* 148 (2007) 560.
4. Mohan and C. U. Pittman Jr., *J. Hazard. Mater.,* 137 (2006) 762.
5. B. Silva, H. Figueiredo, C. Quintelas, I. C. Neves and T. Tavares. *Micropor. Mesopor. Mater.,* 116 (2008) 555.
6. S. Deng and R. Bai. *Water Res.,* 38 (2004) 2424.
7. B. Silva, H. Figueiredo, I. C. Neves and T. Tavares. *World Acad. Sci. Engineer. Techn.,* 43 (2008) 1.
8. C. Max. *Toxicol. Appl. Pharm.,* 188 (2003) 1.
9. Q. Zhang, T. Kluz, K. Salnikow and M. Costa. *Biol. Trace Elem. Res*., 86 (2002) 11.
10. M. R. Hoffmann, S. T. Martin, W. Choi and D. W. Bahnemann. *Chem. Rev.,* 95 (1995) 69.
11. Fujishima, T. N. Rao and D. A. Tryk. *J. Photochem. Photobiol., C* 1 (2000) 1.
12. Linsebigler, G. Lu and J. T. Yates Jr., *Chem. Rev.,* 95 (1995) 735.
13. P. Mohapatra, S. K. Samantaray and K. Parida. *J. Photochem. Photobiol., A* 170 (2005) 189.
14. J. Fang, Z. Zheng, X. Zhaoyi, Z. Shourong, G. Zhaobing and C. Liqiang. *J. Hazard. Mater.,* 134 (2006) 94.
15. Mahata, A. F. Cunha, J. J. M. Orfao and J. L. Figueiredo. *Appl. Catal. A: Gen.,* 351 (2008) 204.
16. Liuyang, Y. Fangli and T. Qing. *Materials Letters,* 62 (2008) 2267.
17. S. Mandal, A. Gole, N. Lala, R. Gonnade, V. Ganvir and M. Sastry. *Langmuir,* 17 (2001) 6262.
18. Z. Zhong, A. S. Subramanian, J. Highfield, K. Carpenter and A. Gedanken. *Chem. A Eur. J.,* 11 (2005) 1473.
19. Z. Ma and H. Han. *Coll. Surf. A: Physicochem. Eng. Asp.,* 317 (2008) 229.
20. Yan, C. Hongling, C. Rizhi and X. Nanping. *Appl. Catal. A: Gen.,* 277 (2004) 259.
21. Y. Kera, H. Kominami, S. Murakami and B. Ohtani. *Photocatal.: Sci. Tech.,* (2003) 29.
22. S. M. Nevskaya, S. A. Nikolaev and E. S. Loktev. Catal. Today, 105 (2005) 344.
23. M. A. Omole, I. O. K'Owino and O. A. Sadik. *Appl. Catal. B: Environ.,* 76 (2007) 158.